Structure and Reactivity of a Mononuclear Non-Haem Iron(III)–Peroxo Complex

Much of the chemistry that is vital for life is performed by metal containing enzymes, and in fact it is these metalloenzymes which allow our bodies to utilize the dioxygen we breathe in and incorporate it into our chemical structure through respiration and other metabolic pathways. For these metalloenzymes to perform their functions, the O-O bond must be split so that a single oxygen atom can be effectively utilized and incorporated into essential biological molecules.

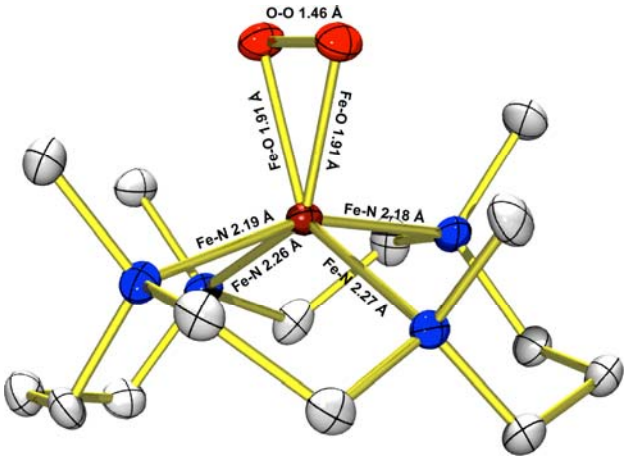

Figure 1. Structure of Fe(III)-peroxo complex, $[Fe(TMC)(OO)]^{+}$. Hydrogen atoms are omitted for clarity. Key bond distances are shown on the structure.

Many of these enzymes are thought to utilize several high-valent intermediates along their reaction coordinates, and in some cases these intermediates have been trapped and studied[1]. To generate these intermediates, metalloenzymes can alter the environment at the metal site, changing the ligation, geometry, the metal-ligand bonds, and oxidation state of the metal. These changes allow the enzyme to perform very difficult and complex chemical reactions under normal biological conditions, chemistry that would otherwise require extreme temperatures and pressures. However, for the vast majority of these metalloenzymes, their highly reactive intermediates remain elusive. As a result, studies on compounds that mimic the structure or function of these reactive sites constitute an attractive area of research for understanding the key chemistry that drives much of the biological reactions.

In this work, Professor Wonwoo Nam's lab at Ewha Womans University in Seoul, South Korea, synthesized three key iron-oxygen reaction intermediates[1-7], an Fe(III)-peroxo, an Fe(III)-hydroperoxo, and an Fe(IV)-oxo species all on a single scaffold of the highly versatile TMC (1,4,8,11-tetramethyl-1,4,8,11-tetraazacyclotetradecane) ligand. These three intermediates where then characterized by the group of Professors Edward Solomon, Keith Hodgson, and Britt Hedman of Stanford University and SLAC using iron K-edge and Extended X-ray Absorption Fine Structure (EXAFS) X-ray Absorption Spectroscopy (XAS) at Stanford Synchrotron Radiation Lightsource Beam Line 9-3 in the fall of 2010. This was significant as generating all intermediates in the same ligand

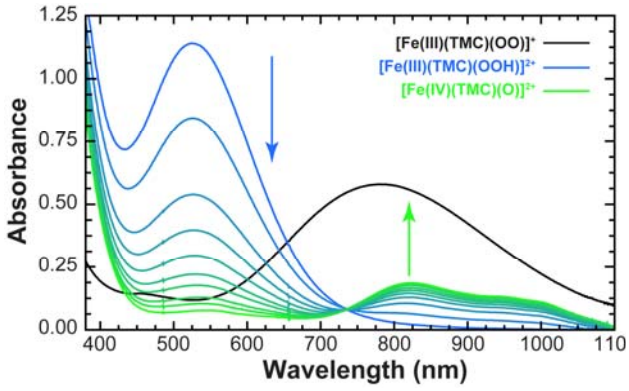

Figure 2. UV-Vis data showing the interconversion from Fe(III)-peroxo (black) to Fe(III)-hydroperoxo (blue) to Fe(IV)-oxo (green). Conversion from Fe(III)-peroxo to Fe(III)-hydroperoxo was very rapid where as from Fe(III)-hydroperoxo to Fe(IV)-oxo took over an hour.

environment allowed this group to study and understand the changes that take place between the iron and the oxygen atoms, irrespective of any changes to the ligand, which is the site of the enzyme that is actually performing the chemistry.

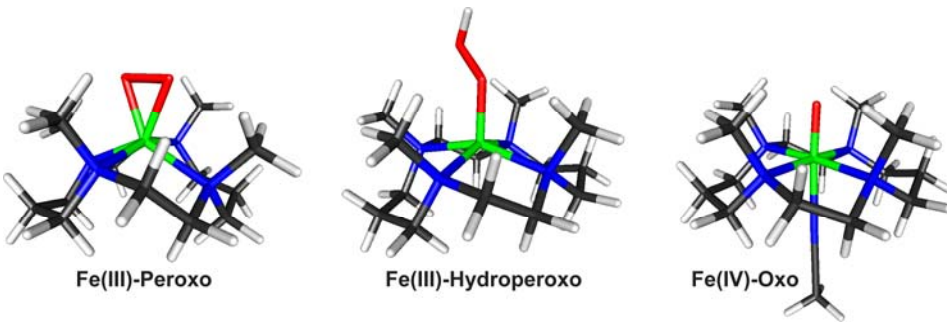

Figure 3. Final EXAFS models for Fe(III)-peroxo, Fe(III)-hydroperoxo, and Fe(IV)-oxo intermediate complexes.

The iron(III)–peroxo complex, was prepared by reacting $[Fe(II)(TMC)(CF_3SO_3)_2]$ with 5 equivalents of H_2O_2 in the presence of 2 equivalents of triethylamine in CF_3CH_2OH at 0 ºC. Remarkably, crystals were grown from this reaction and yielded the first high-resolution crystal structure of a high-valent non-heme fe(III)-peroxo model complex (Figure 1). By adding a slight excess of acid ($HClO_4$), the iron(III)-peroxo complex could then be reversibly protonated to generate a violet intermediate of the iron(III)-hydroperoxo with an electronic absorption band at λ_{max} = 526 nm, which was then followed by slow conversion ($t_{1/2}$ < 60 min) to the corresponding iron(IV)–oxo complex, $[Fe(IV)(TMC)(O)]^{2+}$. (Figure 2).

The XAS data on the three intermediates also characterized a distinct trend of increasing pre-edge intensity across the series from Fe(III)-peroxo to Fe(III)-hydroperoxo to Fe(IV)-oxo (Figure 3). For the Fe(III)-peroxo, these data exhibited a pre-edge intensity which complimented the crystal structure showing that a 6 coordinate high-spin Fe(III)-peroxo species was present. Upon protonation and conversion to the hydroperoxo species, the pre-edge intensity increased showing that the intermediate has undergone a conversion from 6 coordinate to 5 coordinate, likely breaking one of the Fe-O bonds of the side-on peroxo species[8]. Lastly, the Fe(IV)-oxo species exhibited a pre-edge with the largest intensity. This observed pre-edge intensity was consistent with other 6 coordinate Fe(IV)-oxo species characterized in the literature[9-12], and is indicative of the presence of a short and highly covalent Fe=O bond. (Figure 4).

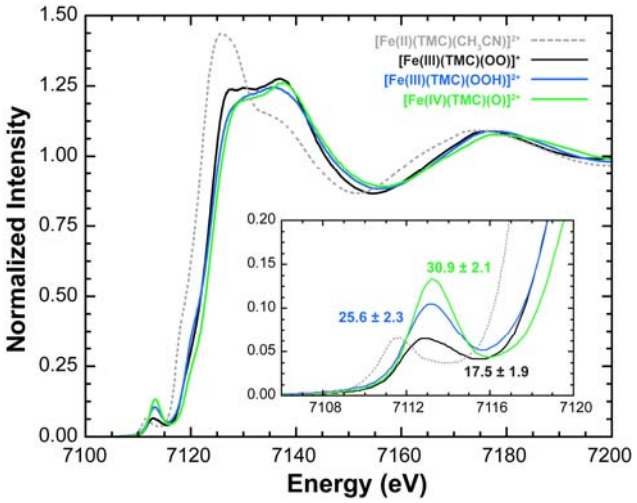

Figure 4. Iron K-edge and pre-edge data (inset) showing the trend of increased pre-edge intensity and changing coordination numbers going from Fe(III)-peroxo, Fe(III)-hydroperoxo, to Fe(IV)-oxo.

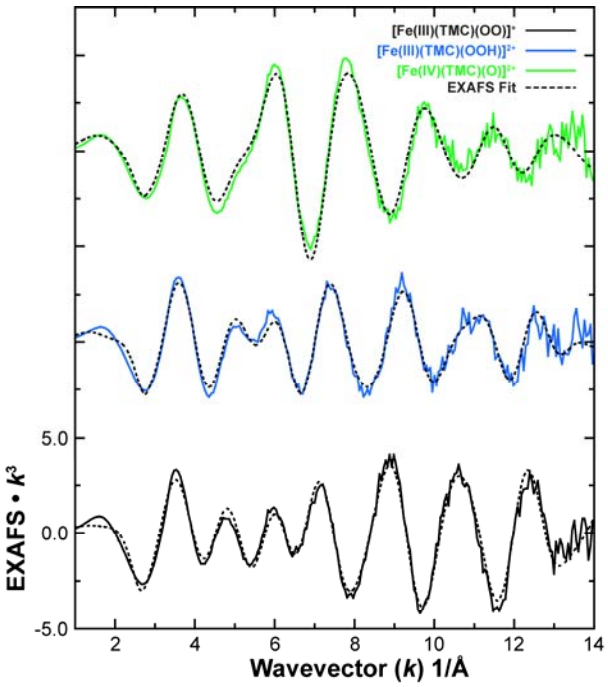

	Path	CN	R(Å)	σ^2 (Å^2)	ΔE_0	Error
Fe(IV)-Oxo						
3-1	Fe=O	1	1.66	520	-3.9	0.71
	Fe-N	4	2.08	395		
3-2	Fe=O	1	1.66	545	-4.2	0.64
	Fe-N	5	2.08	511		
Fe(III)-Hydroperoxo						
2-1	Fe-O	2	1.89	2495	-3.7	0.81
	Fe-N	4	2.17	527		
2-2	Fe-O	1	1.85	526	-1.5	0.72
	Fe-N	4	2.17	584		
Fe(III)-Peroxo						
1-1	Fe-O	1	1.92	86	-0.2	1.05
	Fe-N	5	2.23	582		
1-2	Fe-O	1	1.92	92	-0.6	0.96
	Fe-N	4	2.23	418		
1-3	Fe-O	2	1.92	352	-3.2	0.83
	Fe-N	4	2.22	409		

Figure 5. Left: EXAFS data and final fit for the three intermediates. Notice the distinct difference in the EXAFS waves for each species as caused by changes to the first coordination shell. Right: First shell EXAFS fits showing the changing coordination number.

The EXAFS data also agreed with the Fe K pre-edge results (Figure 5). EXAFS data on the Fe(III)-peroxo intermediate were tested for several coordination environments (Fits 1-1, 1-2, 1-3), with the final fit showing a distinct preference for a 6 coordinate environment with a 2:4 split first shell representing the two Fe-O bonds of the side-on peroxo species and the four additional bonds from the TMC ligand (Fit 1-3); a result consistent with both the crystal structure and the pre-edge observations. Upon protonation, the EXAFS again showed a trend consistent with the pre-edge data, exhibiting a distinct shift to a 1:4 O:N first shell, with no evidence for an axial ligand (Fit 2-2). The 2:4 O:N coordination, which yielded the best fit for the Fe(III)-peroxo EXAFS data was also tested (Fit 2-1), however, this fit resulted in very large bond-variance factors in the first shell, reinforcing the presence of single Fe-O bond in the hydroperoxo species. Lastly, EXAFS fits to the Fe(IV)-oxo showed the presence of a short 1.66Å Fe=O bond, a distance characteristic of this high-valent complex, as well as the addition of an axial ligand showing that the Fe(IV)-oxo complex was 6 coordinate (Fit 3-2). (Figure 5)

In addition to the XAS studies at SSRL, reactivity studies at Ewha Womans University were preformed on all species. These studies showed that of the three species, the Fe(III)-hydroperoxo complex was the most reactive in the nucleophilic deformylation of aldehydes. The Fe(III)-hydroperoxo was also found to have a rate of electrophilic oxidation similar to that of an iron(IV)–oxo complex for C–H bond activation. The Fe(III)-peroxo complex was observed to only be active toward nucleophilic deformylation reactions. These studies successfully characterized and defined the relative reactivity of the three key oxygen intermediates in non-heme iron biochemistry, within the same ligand environment, and their conversion (Figure 6).

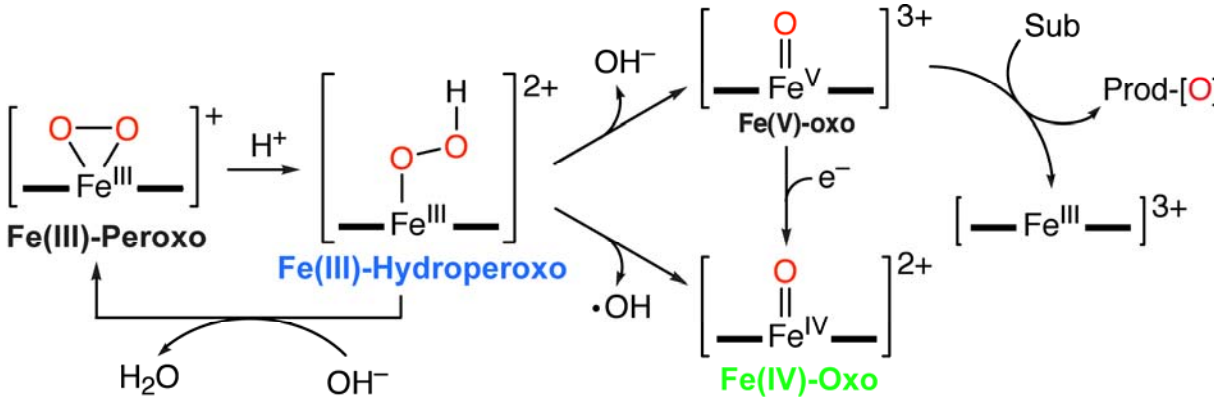

Figure 6: Proposed reaction mechanism of O-O bond cleavage favoring the homolytic cleavage pathway and direct generation of the Fe(IV)-oxo reaction intermediate.

This is the first time this process has been observed and characterized in a high-spin Fe(III)-hydroperoxo species, and marks a significant advance in understanding O-O bond cleavage in both model and metalloenzyme systems. This study was published in *Nature* on October 27th, 2011.

References

1. Karlsson, A.; Parales, J. V.; Parales, R. E.; Gibson, D. T.; Eklund, H.; Ramaswamy, S., Crystal Structure of Naphthalene Dioxygenase: Side-on Binding of Dioxygen to Iron. *Science* **2003,** 299, 1039-1042.
2. Blasiak, L. C.; Vaillancourt, F. H.; Walsh, C. T.; Drennan, C. L., Crystal structure of the non-haem iron halogenase SyrB2 in syringomycin biosynthesis. *Nature* **2006,** 440, 368-371.
3. Cicchillo, R. M.; Zhang, H.; Blodgett, J. A. V.; Whitteck, J. T.; Li, G.; Nair, S. K.; van der Donk, W. A.; Metcalf, W. M., An unusual carbon–carbon bond cleavage reaction during phosphinothricin biosynthesis. *Nature* **2009,** 459, 871-874.
4. Kovaleva, E. G.; Lipscomb, J. D., Crystal Structures of Fe2+ Dioxygenase Superoxo, Alkylperoxo, and Bound Product Intermediates *Science* **2007,** 316, 453-457.
5. Kovaleva, E. G.; Lipscomb, J. D., Versatility of biological non-heme Fe(II) centers in oxygen activation reactions. *Nature Chem. Biol.* **2008,** 4, 186-193.
6. Rittle, J.; Green, M. T., Cytochrome P450 Compound I: Capture, Characterization, and C-H Bond Activation Kinetics. *Science* **2010,** 330, 933-937.
7. Solomon, E. I.; Brunold, T. C.; Davis, M. I.; Kemsley, J. N.; Lee, S.; Lehnert, N.; Neese, F.; Skulan, A. J.; Yang, Y.; Zhou, J., Geometric and Electronic Structure/Function Correlations in Non-Heme Iron Enzymes. *Chem. Rev.* **2000,** 100, 235-350.
8. Westre, T. E.; Kennepohl, P.; DeWitt, J. G.; Hedman, B.; Hodgson, K. O.; Solomon, E. I., A Multiplet Analysis of Fe K-Edge 1s to 3d Pre-Edge Features of Iron Complexes. *J. Am. Chem. Soc.* **1997,** 119, 6297-6314.
9. Lim, M. H.; Rohde, J.-U.; Stubana, A.; Bukowski, M. R.; Costas, M.; Ho, R. Y. N.; Munck, E.; Nam, W.; Que, L., Jr., An FeIVAO complex of a tetradentate tripodal nonheme ligand. *Proc. Natl. Acad. Sci.* **2003,** 100, 3665-3670.
10. Rohde, J.-U.; In, J.; Lim, M. H.; Brennessel, W. W.; Bukowski, M. R.; Stubna, A.; Münck, E.; Nam, W.; Que, L. J., Crystallographic and Spectroscopic Characterization of a Nonheme Fe(IV)¢O Complex. *Science* **2003,** 299, 1037-1039.

11. Rohde, J.-U.; Torelli, S.; Shan, X.; Lim, M. H.; Klinker, E. J.; Kaizer, J.; Chen, K.; Nam, W.; Que, L., Jr., Structural Insights into Nonheme Alkylperoxoiron(III) and Oxoiron(IV) Intermediates by X-ray Absorption Spectroscopy. *J. Am. Chem. Soc.* **2004,** 126, 16750-16761.
12. Yoon, J.; Wilson, S. A.; Jang, Y. K.; Seo, M. S.; Nehru, K.; Hedman, B.; Hodgson, K. O.; Bill, E.; Solomon, E. I.; Nam, W., Reactive Intermediates in Oxygenation Reactions with Mononuclear Nonheme Iron Catalysts. *Angew. Chem. Int. Ed.* **2009,** 48, 1257-1260.

Primary Citation

Cho, J.; Jeon, S.; Wilson, S. A.; Liu, L. V.; Kang, E. A.; Braymer, J. J.; Lim, M. H.; Hedman, B.; Hodgson, K. O.; Valentine, J. S.; Solomon, E. I.; Nam, W., Structure and reactivity of a mononuclear non-haem iron(III)–peroxo complex. *Nature* 2011, 478, 502-505.

Contacts

Samuel Wilson: s4wilson@stanford.edu

Edward I. Solomon: Edward.Solomon@stanford.edu

SSRL is primarily supported by the DOE Offices of Basic Energy Sciences and Biological and Environmental Research, with additional support from the National Institutes of Health, National Center for Research Resources, Biomedical Technology Program, and the National Institute of General Medical Sciences.